

Efficient Variance-reduced Estimation from Generative EHR Models: The SCOPE and REACH Estimators

Luke Solo

University of Chicago

LSOLO@UCHICAGO.EDU

Matthew B. A. McDermott

Columbia University

MM6677@CUMC.COLUMBIA.EDU

William F. Parker

Bashar Ramadan

Michael C. Burkhart

Brett K. Beaulieu-Jones

University of Chicago

WPARKER@UCHICAGO.EDU

BASHARRAMADAN@UCHICAGO.EDU

BURKH4RT@UCHICAGO.EDU

BEAULIEUJONES@UCHICAGO.EDU

Abstract

Generative models trained using self-supervision of tokenized electronic health record (EHR) timelines show promise for clinical outcome prediction. This is typically done using Monte Carlo simulation for future patient trajectories. However, existing approaches suffer from three key limitations: sparse estimate distributions that poorly differentiate patient risk levels, extreme computational costs, and high sampling variance. We propose two new estimators: the Sum of Conditional Outcome Probability Estimator (SCOPE) and Risk Estimation from Anticipated Conditional Hazards (REACH), that leverage next-token probability distributions discarded by standard Monte Carlo. We prove both estimators are unbiased and that REACH guarantees variance reduction over Monte Carlo sampling for any model and outcome. Empirically, on hospital mortality prediction in MIMIC-IV using the ETHOS-ARES framework, SCOPE and REACH match 100-sample Monte Carlo performance using only 10-11 samples (95% CI: [9,11]), representing a $\sim 10\times$ reduction in inference cost without degrading calibration. For ICU admission prediction, efficiency gains are more modest ($\sim 1.2\times$), which we attribute to the outcome's lower "spontaneity," a property we characterize theoretically and empirically. These methods substantially improve the feasibility of deploying generative EHR models in resource-constrained clinical settings.

Data and Code Availability This paper uses the MIMIC-IV dataset (Johnson et al., 2023), which is

available on the PhysioNet repository (Johnson et al., 2016). The empirical experiments in this paper are run on an extended version of the ETHOS-ARES code-base (Renc et al., 2025). This code-base is publicly available on GitHub. All new code, runtime logs, and detailed instructions for how to integrate the new code with the original ETHOS-ARES code-base is publicly available [here](#). In addition, the result files containing the risk scores assigned to each patient are being submitted to the Physionet repository in compliance with their terms for sharing.

Institutional Review Board (IRB) This work performs secondary analysis of de-identified, publicly available data. It was therefore exempt from IRB approval as non-human subjects research.

1. Introduction and Related Work

Existing transformer architectures trained on sequences of tokenized EHR data have been shown to be versatile models that are capable of handling a range of predictive tasks (Li et al., 2020; Rasmy et al., 2021; Wornow et al., 2023b,a; Kraljevic et al., 2024; Waxler et al., 2025). In this framework, the patient's interactions with healthcare are converted from their operational representation (tabular EHR databases) into a sequence of tokens that describe medical events in the patient's timeline, such as labs, vitals, and prescriptions (McDermott et al., 2023; Wornow et al., 2025; Burkhart et al., 2026). These models are then trained using self-supervision with the task of predicting the next token in the patient's timeline. Using

the architecture of the transformer and this next token prediction objective, these models learn context aware representations of tokenized patient timelines.

Once trained, these models can serve as a foundation for patient-level outcome prediction. One class of strategies for doing this involves either extracting the learned intermediate representations from the pre-trained model and training a supervised classifier or performing task-specific finetuning of the full model on labeled timelines (Li et al., 2020; Rasmy et al., 2021; Steinberg et al., 2024, 2021; Guo et al., 2024).

Recently, a second approach has emerged that leverages the generative nature of these models more directly (Renc et al., 2024, 2025). Rather than training on labeled outcomes, the model simulates multiple potential future timelines for each patient, and the proportion of simulated timelines containing the outcome of interest serves as a risk estimate. To enable prediction at specific time horizons, artificial time tokens representing the passage of time are inserted between clinical events (Pang et al., 2021). For example, to estimate a patient’s one-year risk of pancreatic cancer, the model would generate multiple one-year trajectories and report the fraction in which a pancreatic cancer diagnosis token appears.

This type of classifier has a number of advantages over traditional supervised methods. This classifier can be used to generate predictions for an arbitrary number of tasks while re-using the same pool of simulated future timelines. By avoiding task-specific finetuning, these models can generate predictions for new outcomes without re-training a model for each task. Additionally, the output of the classifier is intuitive to clinicians and researchers because results are presented as simulated timelines of the patient’s future.

Despite these advantages, this technique has a number of unique limitations. The primary limitation of this technique is its extreme computational expense. Performing future timeline simulations for new patients demands significantly more computational resources than applying or even training a logistic regression model on the hidden state representations of a sequence. In one of our experiments, performing inference to generate future timelines took more than 8 times longer than the GPU hours used to train the entire next token prediction model. This computational intensity could be a major barrier to prospective clinical deployment, particularly in acute settings such as the intensive care unit (ICU) where risk estimates may need to be refreshed frequently

and with low latency. If inference-time requirements remain high, the method may be limited to offline or low-frequency use rather than real-time decision support.

Additionally, since the predicted probability generated by this method is a proportion of timelines that include the outcome of interest, this method suffers from a dispersion of estimates that limits the range of potential estimates to the rational numbers with a denominator equal to the number of samples. This is especially problematic for rare outcomes. This arithmetic limitation is misaligned with clinical needs: the most consequential decisions are often driven by low-prevalence but high-impact outcomes, where even small absolute differences in low probabilities can meaningfully change diagnostic and therapeutic actions (e.g. evaluating chest or back pain for aortic dissection (Hsia et al., 2016)). For example, even if one were to generate 100 potential future timelines for each patient in a study, which is a standard number currently found in the literature using this technique (Renc et al., 2025), the lowest non-zero likelihood estimate that the model can generate is 1/100. If an outcome of interest has a prevalence of 1/10,000, a patient with true risk 10 times higher than the mean would receive a risk score that exceeds that of an average patient less than 10% of the time (Appendix H). With moderate sample counts, standard Monte Carlo estimates can lack the resolution to separate meaningfully elevated risk from baseline for low-prevalence outcomes, limiting clinical usefulness precisely in high-stakes rare-event settings.

In addition to the problem posed by the dispersion of estimates, this method of generating predictions is limited by the sampling variance itself. Bedi et al. (2026) recently cited sampling variance as a key limitation of these generative model derived predictions that future research must consider. Under the Monte Carlo paradigm, the variance of these estimators will always be equal to $\frac{p(1-p)}{n}$, where p is the probability of the model generating the outcome of interest token and n is the number of sampled timelines. Sampling variance further destabilizes Monte Carlo risk estimates. Separately, the $1/n$ discretization of proportion-based scores introduces stepwise changes in the reported risk. Together, these effects can yield jagged (“stair-stepping”) trajectories when estimates are recomputed over time. For monitoring-style use cases, clinicians benefit from smoother, continuous risk trajectories that better distinguish true physiologic change from sampling noise. The key lim-

itation that keeps the range of the estimates limited and the sampling variance high is the fact that the standard method of generative probability estimation discards valuable information during sequence generation: the probability distribution of next tokens.

In response to encountering this limiting dispersion of estimates problem, [Amar et al. \(2025\)](#) proposed a path-computed probability, similar to our second technique described below, that incorporates the probability of generating the outcome of interest token at each step in order to produce an estimator that resolved the dispersion of estimates problem for their model. However, their manuscript does not specify whether or not the outcome of interest token is sampled for the timelines that comprise these paths. If they do include the outcome of interest during sampling, their method is a biased estimator that is a worse version of our second estimator REACH. If they do exclude the outcome of interest token during sampling, their method is mathematically equivalent to our second estimator. Also, since this method was not the primary focus of the paper, important statistical properties of the estimator, such as unbiasedness and whether or not the estimator had lower variance than the MC estimator, were neither explored nor demonstrated.

In light of both the promise and the limitations of the standard Monte Carlo method, we propose two new estimators: Sum of Conditional Outcome Probability Estimates (SCOPE) and Risk Estimation from Anticipated Conditional Hazards (REACH). We provide a derivation, a proof of unbiasedness, and a rigorous characterization of the variance for both estimators. These theoretical results are reinforced by synthetic experiments on Markov chains, which help illustrate the conditions under which these methods offer the greatest reductions in variance, and an implementation in the ETHOS-ARES framework, where the performance of these new methods are compared to the Monte carlo method on the tasks of hospital mortality and ICU admission.

2. Description of Estimators

2.1. Introduction of Notation

Let P be a distribution for the next token drawn from some vocabulary of tokens V , which can be conditioned on some timeline of generated tokens $X_{1:i}$. We define a random variable T_O that denotes the first index at which some designated outcome of in-

terest token $O \in V$ appears in a given sequence, or ∞ if the token does not appear in the timeline. We represent the calendar time passing for a tokenized timeline $X_{1:i}$ with a time-token generating function $\mathcal{T} : V \rightarrow \mathbb{R}$, which maps artificial time tokens to their specified times and all other tokens to zero. Then, the time of the token at index j is equal to $\sum_{k=1}^{j-1} \mathcal{T}(X_k)$. The notation \hat{X} is also used throughout the text to refer to a tokenized timeline that was generated under an alternative probability distribution \hat{P} , where the probability of generating the outcome of interest token O has been set to zero. We also define a second random variable T_E as the minimum between: the index of the first token with a timestamp that exceeds some given time threshold and the index of the first token that is in some subset of tokens that are considered sequence-terminating. Intuitively, this can be thought of as the end of the patient’s timeline. Although it is pragmatic in many real world simulations to stop inference when the outcome of interest token O is generated, for the sake of our notation and proofs, $T_E \neq T_O$, and if the outcome of interest is sequence terminating, let $T_E = T_O + 1$ by convention. In this work, T_E is taken to be finite for all sequences in the support of P . This probability space and these random variables establish a rigorous framework for next token predicting models that are used to predict future medical timelines over a limited time horizon.

2.2. Standard Monte Carlo Generation μ

$$M_0 = \frac{1}{n} \sum_{i=1}^n \mathbb{1}_{\{T_O(X^{(i)}) < T_E(X^{(i)})\}} \quad (1)$$

The most straightforward way to leverage a generative event model to estimate the probability of a given outcome occurring is to perform a Monte Carlo sampling of future timelines. By randomly generating n future timelines, a simple and unbiased estimator for the probability of an outcome can be derived by computing the proportion of timelines that include this outcome, defined rigorously in (1). The most expensive step required for this method is the simulation of future timelines. For our ETHOS-ARES experiments, training the next token generation model took less than 192 GPU hours. Inference for the hospital mortality task, on the other hand, required an estimated 1,537 GPU hours under the default ETHOS-ARES settings. However, since these timelines are generated identically regardless of which outcome of interest one hopes to quantify, a single pool of sam-

pled timelines can be re-used to generate probabilities for as many outcomes as desired.

Additionally, this technique permits a broader range of outcome definitions than the following two methods, which are only defined for outcomes that can be expressed as a single token. However, this technique is hindered by a rigid and sparse potential output space, which creates a dispersion of estimates problem described above.

2.3. Sum of Conditional Outcome Probability Estimates (SCOPE)

$$\mathcal{S} = \frac{1}{n} \sum_{i=1}^n \left[\sum_{t=1}^{\min\{T_E(X^{(i)}), T_o(X^{(i)})\}} P(X_t = O | X_{1:t-1}^{(i)}) \right] \quad (2)$$

The Sum of Conditional Outcome Probability Estimates method, referred to as \mathcal{S} in equations, begins with the same process as the Monte Carlo method: our model generates a pool of potential future timelines. However, where the above method fails to use any information about the next token distribution at each step, this method computes an unbiased estimate by taking a sum of the probabilities that the next token is the outcome of interest token. This sum terminates at either the end of the timeline or when the outcome of interest token is selected as the next token. Just by saving the next token distribution, an often negligible memory cost, this estimator can be computed using the same pool of reusable sampled timelines as the Monte Carlo method.

Since each sub-estimator is a sum of next token probabilities, the potential values of the overall estimator are much more continuous than those of the Monte Carlo estimator. However, since the values for this estimator are a sum of raw probabilities, there are situations where the estimator can produce a value above 1. In situations where this is more probable, the variance of this estimator can exceed the variance of the MC method. Additionally, this introduces the following double bind. If SCOPE predictions are not clipped to fall in the $[0, 1]$ range, they are not valid probability estimates. However, if they are clipped to this range, SCOPE is no longer guaranteed to be an unbiased estimator. Despite these concerning potential limitations, in both empirical tasks using real world data with 43,047 patients with 100 timelines each, not one timeline provided a SCOPE sub-estimator that exceeded 1.0.

2.4. Risk Estimation from Anticipated Conditional Hazards (REACH)

$$\mathcal{R} = \frac{1}{n} \sum_{i=1}^n \left[1 - \prod_{t=1}^{T_E} (1 - P(X_t = O | \hat{X}_{1:t-1}^{(i)})) \right] \quad (3)$$

Unlike the two above methods, Risk Estimation from Anticipated Conditional Hazards, which is referred to as \mathcal{R} in equations, samples timelines where the outcome of interest token is **excluded** from the pool of possible next token candidates. These outcome-free timelines are then used as a backbone for a discrete time survival process. After the i th token in a generated timeline, if the model assigns probability h_i to the possibility that the next token is the outcome of interest, we can treat each step as a survival process where our simulated patient progresses to the next token with probability $1 - h_i$ and experiences the outcome of interest with probability h_i . The probability that the patient experiences the outcome of interest given this backbone is then equal to the inner term in the above sum.

This estimator eliminates the variance incurred by the model deciding whether or not the outcome of interest actually occurs. As a result, REACH is proven to be a lower variance unbiased estimator than both of the techniques described above. The primary limitation of this method is that outcome-free backbone timelines are not able to be used for other predictive tasks since they forbid the outcome of interest token from appearing.

2.5. Theoretical Guarantees

For the methods described above, we provide proofs for the following important facts about \mathcal{S} and \mathcal{R} .

- \mathcal{S} and \mathcal{R} are unbiased estimators of the probability of the outcome of interest token being generated
- \mathcal{R} is guaranteed to have variance less than or equal to the variance of both the MC and \mathcal{S} methods
- Even in the event of model mis-specification, \mathcal{R} is guaranteed to have MSE no greater than that of the MC and \mathcal{S} methods

3. Proofs

3.1. Derivation and Unbiasedness of \mathcal{S} (SCOPE)

In addition to the random variables introduced above, let X be a random variable equal to the sequence of

tokens iteratively drawn from the next token distribution P :

$$\begin{aligned}\mathbb{P}(T_O < T_E) &= \mathbb{E}_{X \sim P} [\mathbb{1}_{T_O(X) < T_E(X)}] \\ &= \mathbb{E}_{X \sim P} [\sum_{t=1}^{\infty} \mathbb{1}_{\{T_O(X)=t\}} \mathbb{1}_{\{T_E(X)>t-1\}}]\end{aligned}$$

Equivalent to the product of the indicator r.v.s in the interior of the term above, to simplify the notation, define a new function f over partial sequences:

$$\begin{aligned}g(x_{1:t-1}) &= \mathbb{1}_{\{O \notin x_{1:t-1}\}} \mathbb{1}_{\{T_E(x_{1:t-1}) > t\}} \\ f(x_{1:t}) &= \mathbb{1}_{\{x_t=O\}} g(x_{1:t-1})\end{aligned}$$

Note that for any sequences exceeding the time horizon or containing O , the above function will map to zero. So that, by the linearity of expectation and the law of total expectation:

$$\begin{aligned}\mathbb{P}(T_O < T_E) &= \sum_{t=1}^{\infty} \mathbb{E}_{X \sim P} [f(X_{1:t})] \\ &= \sum_{t=1}^{\infty} \mathbb{E}_{X_{1:t-1} \sim P} [\mathbb{E}[f(X_{1:t}) | X_{1:t-1}]] \\ &= \sum_{t=1}^{\infty} \mathbb{E}_{X_{1:t-1} \sim P} [g(X_{1:t-1}) \mathbb{E}[\mathbb{1}_{\{x_t=O\}} | X_{1:t-1}]] \\ &= \sum_{t=1}^{\infty} \mathbb{E}_{X_{1:t-1} \sim P} [g(X_{1:t-1}) \mathbb{P}(X_t = O | X_{1:t-1})]\end{aligned}$$

Next by the law of total expectation

$$\begin{aligned}\mathbb{E}_X (g(X_{1:t-1}) \mathbb{P}(X_t = O | X_{1:t-1}) | X_{1:t-1}) \\ &= \mathbb{E}_{X_{1:t-1}} [\mathbb{E}[g(X_{1:t-1}) \mathbb{P}(X_t = O | X_{1:t-1}) | X_{1:t-1}]] \\ &= \mathbb{E}_{X_{1:t-1}} [g(X_{1:t-1}) \mathbb{P}(X_t = O | X_{1:t-1})]\end{aligned}$$

Substituting this into the above

$$\begin{aligned}\mathbb{P}(T_O < T_E) &= \sum_{t=1}^{\infty} \mathbb{E}_{X \sim P} [g(X_{1:t-1}) \mathbb{P}(X_t = O | X_{1:t-1})] \\ &= \mathbb{E}_{X \sim P} [\sum_{t=1}^{\infty} g(X_{1:t-1}) \mathbb{P}(X_t = O | X_{1:t-1})] \\ &= \mathbb{E}_{X \sim P} [\sum_{t=1}^{\min\{T_E(X), T_O(X)\}} \mathbb{P}(X_t = O | X_{1:t-1})]\end{aligned}$$

The inside of this expression, which we will denote S_i , can then be sampled to generate an unbiased estimator, $\mathcal{S} = \frac{1}{n} \sum_{i=1}^n S_i$.

3.2. Characterization of the Variance of \mathcal{S}

By the fact that each sample is i.i.d., $\text{Var}(\mathcal{S}) = \text{Var}(S)/n$. Therefore by the variance of a Monte Carlo estimator, letting $\mu = \mathbb{E}(\mathcal{S}) = \mathbb{E}(M_0)$:

$$\begin{aligned}\text{Var}(\mathcal{S}) - \text{Var}(M_0) &= \frac{\text{Var}(S) - \mu(1 - \mu)}{n} \\ \text{Var}(\mathcal{S}) - \text{Var}(M_0) &= \frac{\mathbb{E}(S^2) - \mu^2 - \mu + \mu^2}{n} \\ \text{Var}(\mathcal{S}) - \text{Var}(M_0) &= \frac{1}{n} \mathbb{E}[S(S - 1)] \\ \text{Var}(\mathcal{S}) < \text{Var}(M_0) &\iff \mathbb{E}[S(S - 1)] < 0\end{aligned}$$

Note that if $S < 1$ with probability 1 then this statement is always true. However, for any timeline where there are sufficiently many tokens where the probability of the outcome of interest is sufficiently high, S will indeed exceed 1. This means that \mathcal{S} is not

necessarily a lower variance estimator than M_0 and should therefore be checked as an alternative for M_0 rather than a universal replacement. Additionally, since S is more likely to be large for more probable events, since it is an unbiased estimator for μ , \mathcal{S} is often a higher variance estimator than M_0 for experiments where the outcome of interest appears with higher probability, which is reflected in our synthetic and empirical results. However, as is shown in the appendix, $\text{Var}(\mathcal{S}) > \text{Var}(M_0)$ can hold for arbitrarily low mean. Fortunately, the additional computational cost required to compute both M_0 and \mathcal{S} for a given outcome is limited to saving and summing the probabilities, which is negligible when compared to the computational cost of inference.

3.3. Derivation and Unbiasedness of \mathcal{R} (REACH)

Moving to a study of the second new estimator, \mathcal{R} , we define the probability space Ω_{M_τ} as the probability space containing all future timelines generated according to some next token distribution generating model M and time limit τ (where each token is assigned a time value and generation terminates when the sum of all time values exceeds the time limit). This mirrors the standard next token inference.

Within this space, the event A is the subset of all timelines that, at some point before the end of the timeline, contain some outcome of interest token O . From this, we can naturally define a Monte Carlo estimator for $P(A)$ by sampling m timelines and using the fraction of samples that include the outcome of interest token as an unbiased estimate of $P(A)$. Note that by our definition in methods, M_0 as in (1) is simply the result of sampling $\mathbb{1}_A$ and taking the arithmetic average.

Moving beyond the traditional paradigm, we can define a second probability space $\Omega_{\mathcal{O}}$. Timelines are generated using the same model and time limit as in the previous probability space; however, in this probability space, we set the probability of the next token being the outcome of interest token to zero and re-normalize the other probabilities to add to one. Additionally, for each new token in our potential future timeline, we perform a Bernoulli trial with probability of success equal to the probability that the outcome of interest token would have been generated at this token under the original paradigm.

Similarly to how we defined the event A , we can define the event B as the subset of the probability

space where at least one of the Bernoulli trials along the timeline was a success. It is shown in detail in the appendix that $P(A) = P(B)$. This is shown by constructing the natural bijection between the complements A^C and B^C where each timeline in A^C , which must by definition be outcome-free, is mapped to the element in B^C with an identical timeline and a series of Bernoulli trials where all are failures. This bijection preserves probabilities, and the law of total probability then ensures $P(A) = P(B)$.

By the tower rule, $P(B) = \mathbb{E}(\mathbb{1}_B) = \mathbb{E}_{\hat{X}_{1:n}}(\mathbb{E}(\mathbb{1}_B|\hat{X}_{1:n}))$, so $\mathbb{E}(\mathbb{1}_B|\hat{X}_{1:n})$ is an unbiased estimator for $P(A)$ for any sampled timeline $\hat{X}_{1:n}$. Since $\mathbb{1}_B|\hat{X}_{1:n}$ is simply the event that at least one Bernoulli trial succeeds, it is clear that

$$\mathbb{E}(\mathbb{1}_B|\hat{X}_{1:n}) = 1 - \prod_{t=1}^{T_E} (1 - P(X_t = O|\hat{X}_{1:t-1}))$$

which reveals that our estimator \mathcal{R} is in fact equivalent to the average of taking samples of $\mathbb{E}(\mathbb{1}_B|\hat{X}_{1:n})$ and is therefore an unbiased estimator for the probability that a sampled timeline will contain the outcome of interest token.

3.4. Characterization of the Variance of \mathcal{R}

Letting m_0 be the samples that determine M_0 and R be the samples that determine \mathcal{R} , by the law of total variance:

$$\begin{aligned} \text{Var}(M_0) &= \frac{1}{n} \text{Var}(m_0) = \frac{1}{n} \text{Var}(\mathbb{1}_A) = \frac{1}{n} \text{Var}(\mathbb{1}_B) \\ &= \frac{1}{n} (\mathbb{E}(\text{Var}(\mathbb{1}_B|\hat{X}_{1:n})) + \text{Var}(\mathbb{E}(\mathbb{1}_B|\hat{X}_{1:n}))) \\ &= \frac{1}{n} (\text{Var}(\mathcal{R}) + \mathbb{E}(\text{Var}(\mathbb{1}_B|\hat{X}_{1:n}))) \\ &= \text{Var}(\mathcal{R}) + \mathbb{E}(\text{Var}(\mathbb{1}_B|\hat{X}_{1:n}))/n \end{aligned}$$

so that:

$$\text{Var}(M_0) - \text{Var}(\mathcal{R}) = \mathbb{E}(\text{Var}(\mathbb{1}_B|\hat{X}_{1:n}))/n. \quad (4)$$

This also implies that $\text{Var}(\mathcal{R}) \leq \text{Var}(M_0)$. Since $\mathbb{1}_B|\hat{X}_{1:n}$ is simply an indicator random variable, the variance is equal to $p(1-p)$ where p is the probability of one of the Bernoulli trials changing a token to the outcome of interest token at any point along the outcome-free timeline. Intuitively, this means that \mathcal{R} presents a larger improvement to M_0 in scenarios in which an outcome-free timeline has a higher degree of uncertainty regarding the outcome of interest, with the difference becoming larger the closer p is to 0.5.

Note that \mathcal{R} is strictly lower variance than M_0 if $\mathbb{E}(\text{Var}(\mathbb{1}_B|\hat{X}_{1:n})) > 0$, which is always true if there exists a single timeline with non-zero probability where $p \notin \{0, 1\}$. Thus, we have shown that \mathcal{R}

is an unbiased estimator for the true probability that the outcome of interest token will be generated and that \mathcal{R} is a lower variance estimator than the Monte Carlo estimator.

In addition to being a lower variance estimator than the Monte Carlo method, \mathcal{R} is also a lower variance estimator than \mathcal{S} for all models and stopping conditions. This fact is demonstrated in detail in the appendix. Finally, since all three estimators are unbiased and \mathcal{R} has variance no greater than M_0 and \mathcal{S} , it follows directly from the bias variance decomposition of the mean squared error, $MSE(\hat{\theta}) = (\mathbb{E}[\theta - \hat{\theta}])^2 + \text{Var}(\hat{\theta})$, that \mathcal{R} has MSE no greater than either of the other estimators.

4. Experimental Methods

4.1. Markov Chain Experiments

In order to measure how the theoretical guarantees of these techniques translate to actual improvements in the accuracy of generative event model derived predictors, we first implement a suite of Markov Chain synthetic experiments that allow us to analyze the properties of these new estimators in an easily controlled and computationally cheap manner. Under this framework, the next token distribution relies only on the most recent token, rather than the entire sequence of tokens. For these experiments, we reduce the generative event model timeline simulation paradigm of “Generate next tokens until a certain time limit or terminal condition” to “Progress in the discrete time Markov chain until a specified number of steps have been taken”. And, standing in for a clinically significant token, we choose one state in the chain to act as the “outcome of interest” and use our two new methods and the traditional Monte Carlo method to estimate the probability of reaching this “outcome of interest” state.

One important statistic that we define for these random Markov chains is **spontaneity**. In these experiments, the spontaneity of a Markov chain is equal to the proportion of states that have non-zero transition probability to the outcome of interest. This variable is important in understanding which predictive tasks SCOPE and REACH will provide the greatest advantage and this importance is also reflected in our proofs and real world data experiments.

4.2. Empirical Implementation Using ETHOS-ARES

Beyond theoretical guarantees and simplified experiments, it is most important to study how successful these methods are in contributing to the generation of accurate predictions on real world patient data. To this end, we added implementations of both of our new prediction methods to the existing [ETHOS-ARES code base](#), originally published by [Renc et al. \(2025\)](#). By using the ETHOS-ARES code base, we can assess the efficacy of these techniques in a model that has already demonstrated strong generation based predictive capabilities. Using this model, we hope to answer two primary questions. First, what factor of reduction in required inference samples does each technique require to match the performance of the Monte Carlo method? Second, how do these methods affect the calibration of these models in practice? And finally, does the implementation of these methods generate a statistically significant improvement in prediction accuracy when using the full pool of inference samples?

For this empirical testing, we reproduced the entire MIMIC-IV 3.1 ETHOS-ARES pipeline to create a cohort of EHR patients, generate tokenized timelines for these patients, and predict various outcomes for these patients. In order to ensure a fair comparison between the original Monte Carlo method and our new methods, the original machine learning pipeline presented in the paper was preserved and reproduced in as many respects as possible. Notably, this includes the decision not to disable dropout during timeline inference, which is not explicitly mentioned in either [Renc et al. \(2024\)](#) or [Renc et al. \(2025\)](#) but is demonstrated by the fact that eval mode is not enabled for the model during inference.

However, in order to overcome the excessive expected inference times, the inference methods presented in the original ETHOS-ARES database were significantly overhauled with the aim of reducing the computational cost. First, KV caching was added to their inference methods in order to significantly reduce inference times. Additionally, since the ETHOS-ARES model uses a fixed-length sliding context window, it was necessary to add a skip size parameter, which determined how many tokens the sliding context window would jump when the timeline reached the maximum length, in order to preserve the speedups offered by KV caching for sequences that exceed the maximum context length. For this

parameter, a skip size of 64 was selected as it was the lowest parameter tried that preserved the substantial speedup offered by KV-caching. These changes resulted in a roughly nine fold decrease in inference time. The specific run-times used to generate this estimate can be found in the log files of the code supplement and are listed in [Appendix\(E\)](#). The code for these modified inference methods can be found in the GitHub repository.

100 total timelines are sampled for all combinations of the two predictive tasks: hospital mortality and ICU admission as defined in [Renc et al. \(2025\)](#), and all three estimators. Note, since SCOPE and the Monte Carlo method are both derived from usually sampled timelines, the same pool of timelines is used to compute both estimators. After all timelines are finalized, the AUROC for each method on each predictive task is computed. Additionally, in order to understand the performance of these estimators as the number of samples varies, AUROC scores are computed for each task-method combination at a variety of different sample counts. Note that for this experiment no new timelines are computed. Instead, timelines are sampled from the original 100. In order to achieve stable results, this sub-sampling is bootstrapped 40 times and the average AUROC appears in the first plot. Finally, in addition to examining the relationship between number of samples and AUROC, the calibration curves of each of the task-method combinations will be plotted in order to assess the effect, if any, each method has on the quality of calibration achieved by the model.

Furthermore, to better illustrate the reductions in inference time these methods enable, an additional plot is provided that compares the number of samples provided to the Monte Carlo estimator to the minimum number of samples required for the other methods to exceed this performance. For the sake of clarity, this equivalence is presented as a ratio of the form $\frac{\text{Number of MC samples}}{\text{Number of other estimator samples}}$. Intuitively, it can be understood as the number of MC samples for every 1 sample of the alternative estimator. In order to generate confidence intervals, 40 AUROC values from a given sample size for each of the novel estimators are sampled with replacement from the total pool of 40 to compute a mean AUROC for all combinations of novel estimator and sample size. These values are then compared to the mean AUROC of the Monte Carlo method at each sample size. The result of each bootstrap is that each sample size n is assigned an equivalence number m , where m is the smallest sam-

ple size at which $\text{AUROC}(m) > \text{AUROC}(n)$. This allows us to generate confidence intervals for the equivalence ratio m/n at all sample sizes n between 1 and 100.

5. Results

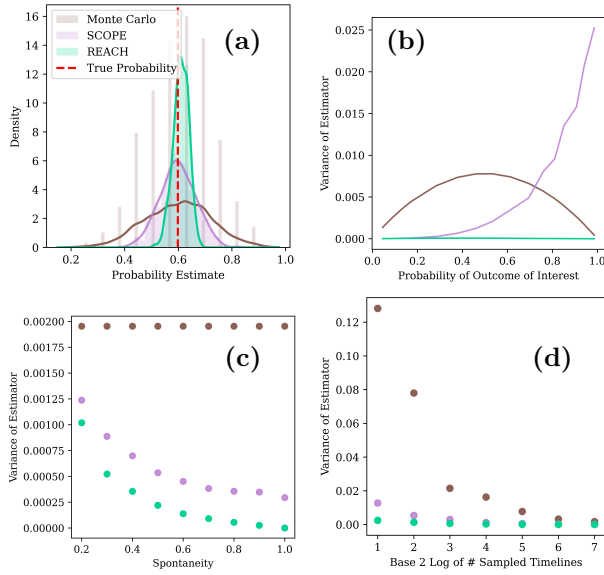


Figure 1: (a) Distribution of estimators vs true probability. (b) Variance of Estimator vs Probability. (c) Variance vs Spontaneity. (d) Variance vs Number of Sampled Timelines.

5.1. Markov Chain Synthetic Experiments

Having rigorously demonstrated important facts about SCOPE and REACH, we now use Markov chains to demonstrate the empirical impact of these estimators and study how well these new estimators perform under specific model and task configurations. Note: All figures presented in this section were generated using the default parameters of 4 experiments in the Markov chain notebook.

These experiments reinforce many of our empirical results, while also hinting at new important insights. Figure 1(a) visually demonstrates the way in which both SCOPE and REACH resolve the dispersion of estimates problem, which can be seen in the fully separated spikes of the Monte Carlo estimator’s distribution. REACH and SCOPE also show a significant reduction in variance over the Monte Carlo estimator.

In Figure 1(b), the relationship between the variance of SCOPE and REACH and the probability of the outcome of interest is clearly shown. For

lower true probabilities, the variance of SCOPE is extremely low and is not visibly different from that of REACH. However, as the true probability grows, and with it the probability of \mathcal{S} producing sampled values that exceed 1, the variance of SCOPE grows very rapidly and exceeds that of the MC estimator when the probability of the outcome of interest is above 0.8. Additionally, in this graph, the variance of REACH is practically zero. This is because, for the Markov chain used to generate this figure, the spontaneity is 1.0, or, in other words, every state is capable of transitioning to the outcome of interest. This leaves a high degree of uncertainty regarding whether or not the outcome of interest will occur based on the outcome free backbone alone, which, by (4), means that REACH will generate the most considerable reduction in variance. This result is also reflected later in Figure 1(d).

Next, Figure 1(c) reflects the way in which the difference in variance between REACH and the MC estimator depends on the uncertainty of the non-outcome timelines. The Markov chains for this figure are uniquely determined by fixing both the probability of reaching the outcome of interest at 0.5, specifying a number of states that can reach the outcome of interest, and assigning all non-outcome states equal transition probability to all other non-outcome states. By fixing the probability of generating the outcome of interest token, we fix the variance of the Monte Carlo method, allowing us to better assess how the difference between the variance of the MC method and our methods varies as spontaneity varies.

Recall that spontaneity is a measurement of the fraction of states in the Markov chain that have non-zero transition probability to the outcome of interest. When spontaneity is low, there are a small number of states that can transition to the outcome of interest. On the other hand, as the spontaneity increases and nearly all timelines have non-zero transition probability to the outcome of interest, the variance of the SCOPE and REACH estimators approach zero while the variance of the Monte Carlo estimator remains stable. Therefore, the frequency with which these states appear in the non-outcome timeline primarily determines the probability calculated from that timeline. Thus, events and outcomes which appear in tokenized timelines most spontaneously will benefit most noticeably from the implementation of REACH. Although not directly implied by our earlier work, a similar relationship seems to hold between SCOPE and the MC estimator.

Finally, Figure 1(d), which is closely reflected experimentally in Figure 2(a), examines the performance of all three methods under varying numbers of samples. Note that the x axis is in log base 2 scaling.

5.2. ETHOS-ARES Empirical Results

Beyond the abstract understanding of these estimators offered by our proofs and Markov chain experiments, the ETHOS-ARES experiments examine the effectiveness of these novel estimators on real world tasks and data. Figures 2(a) and 2(i) show that, using only about 11 (95% CI: [11, 11]) predicted future timelines for SCOPE and 10 (95% CI: [9, 11]) for REACH, both methods matched the performance of the Monte Carlo estimator that utilized 100 predicted timelines for the task of predicting hospital mortality. This represents a drastic reduction in the amount of computational resources required to compute such estimates. Furthermore, this reduction in the required inference for equivalent performance becomes even more dramatic with lower sample counts. With 40 or fewer sampled timelines, Monte Carlo fails to match the performance of either SCOPE or REACH using only 1 sampled timeline.

Although much less dramatic than in the hospital mortality task, 2(c) and 2(ii) still show both SCOPE and REACH offer improvements in predictive accuracy over the Monte Carlo estimator at all sample counts when predicting ICU admission, with SCOPE matching 100 sample performance with only 89 (95% CI: [88, 90]) and REACH achieving the same in only 82 (95% CI: [81, 83]). Just as in the case of hospital mortality, the ratio of samples increases with smaller reference sample counts, with Monte Carlo requiring 5 samples to best the performance of both estimators with only 1 timeline.

For both of the above tasks, 2(b) and 2(d) demonstrate that there is no significant degradation in the quality of the calibration in either predictive task. Additionally, for all combinations of task and estimator except for SCOPE on hospital mortality with 10 samples, there were no statistically significant differences in Brier scores of the Monte Carlo method using 100 samples compared to the equivalent sample counts presented above, and, although statistically significantly worse, the Brier score of the 10-sample SCOPE estimate on hospital mortality is not meaningfully different from the Monte Carlo 100-sample score (0.016 vs 0.015).

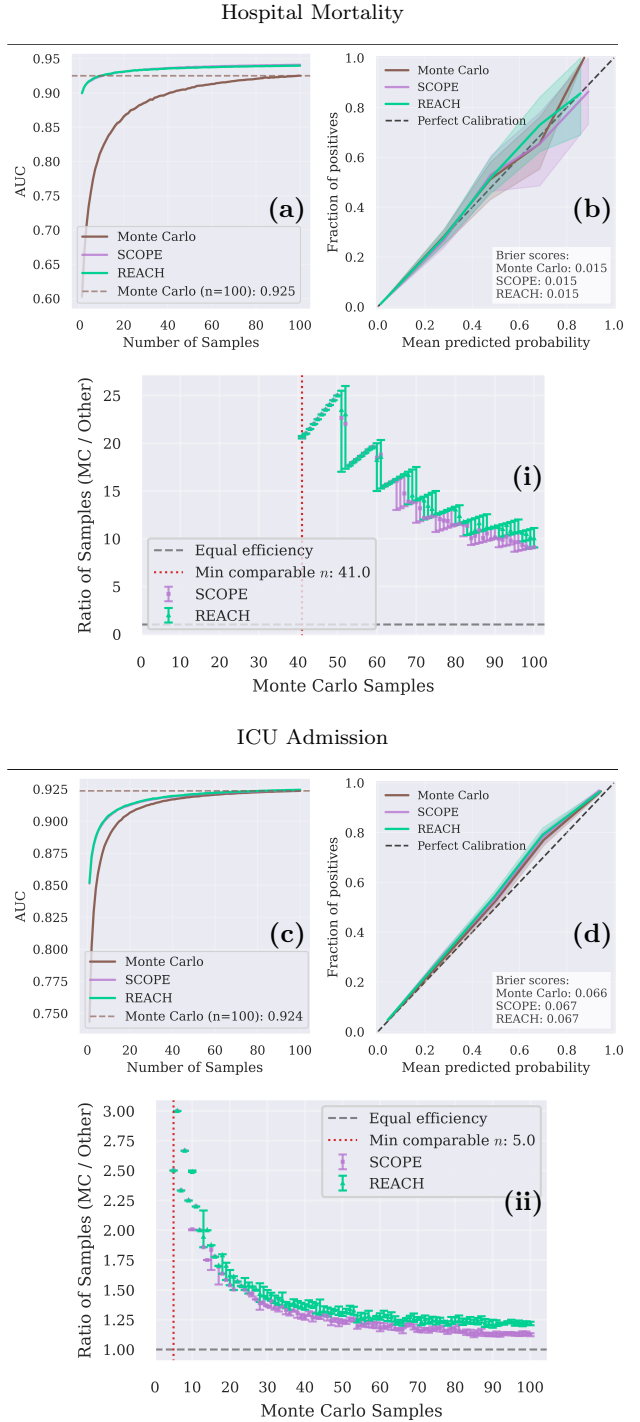


Figure 2: (a) Hospital Mortality AUC vs number of sampled timelines. (b) Hospital Mortality calibration curves (100 samples for all estimators). (c) ICU Admission AUC vs number of sampled timelines. (d) ICU Admission calibration curves (100 samples for all estimators).

The discrepancy between the impact of SCOPE and REACH in these two tasks can, in part, be under-

stood as a result of the “spontaneity” of each task, reflected in Figure 1(c). Depending on the tokenization process, mortality can be a rather sudden event in a patient timeline, and it will therefore continuously carry some ambient probability of being the next token based on the risk suggested by the past timeline. On the other hand, clinician initiated actions such as ICU admission are precipitated by clinical information that should be present in the tokenized timeline. So, by (4), this would suggest that the improvement over the Monte Carlo method would be less significant, since the outcome free tokenized timeline would be much less uncertain. For future work, this suggests that the greatest benefit of these methods will be found on tasks that involve a greater degree of spontaneity. In addition to spontaneity, ICU admission is a much more prevalent outcome than mortality (15.44% vs 1.85%, [Renc et al. \(2025\)](#)). This means that resolving the dispersion of estimates problem is much less meaningful than it is for a rarer event, like hospital mortality.

6. Conclusion

From these results, both empirical and theoretical, it is clear that SCOPE and REACH are not only capable of resolving the dispersion of estimates problem that currently hinders generative outcome prediction but that they also are capable of matching the predictive accuracy of the Monte Carlo method while sampling a much smaller number of potential future timelines. In particular, since REACH offers provably guaranteed lower variance than the MC method, it should be the preferred estimator estimator in situations where only one outcome of interest is of concern. On the other hand, since SCOPE can be computed without additional inference time, these strong empirical results suggest that SCOPE should consistently be considered as an alternative to the standard Monte Carlo method. In addition to demonstrating the promise of these methods, these results also illustrate which types of predictive tasks are likely to gain the most from the implementation of these methods: prediction of rare or “spontaneous” events, for which the patient’s history describes a risk rather than a guarantee.

Ultimately, these improvements better align generative outcome prediction with practical clinical constraints. By reducing inference cost, they make lower-latency and more frequent risk updates more feasible. By improving resolution in the low probabil-

ity regime, they support decision-making for rare but consequential events. Finally, by producing continuous risk estimates, they can yield smoother and more interpretable trajectories than stepwise Monte Carlo proportions, helping clinicians separate physiologic change from sampling noise.

6.1. Limitations

However, there are limitations to both these estimators and this study that must be considered in future work. As demonstrated above both theoretically and experimentally, SCOPE can produce worse variance estimators for the outcome of interest probability than the Monte Carlo method under certain conditions, which are more likely when the outcome of interest is more probable. On the other hand, although REACH is guaranteed to act as a lower variance estimator than either the traditional method or SCOPE, REACH requires the selection of an outcome of interest prior to timeline inference, which means that the sampled timelines are not reusable for additional predictive tasks. This makes REACH a less favorable choice of estimator if a large number of predictive tasks are to be considered. Additionally, both estimators require that the outcome of interest is captured by the appearance of a single token, which might not be possible for all predictive tasks. And finally, the empirical portion of this study only utilizes Markov Chain synthetic examples and two tasks within the ETHOS-ARES codebase.

6.2. Future Work

Since these estimators provide continuous risk scores for patient timelines, rather than binary labels of whether or not the outcome of interest token was observed, these methods could potentially be used to improve clinician understanding of generative event models by identifying common events or features of high risk timelines. Furthermore, not only are these risk scores continuous at the whole timeline level, but for REACH in particular, the risk scores evolve over time, which could provide clinicians with clearer intuition regarding the trajectory of a patient with respect to specific outcomes. This potential for the construction of foundation model derived survival curves has a large number of potentially valuable applications.

References

Jonathan Amar, Edward Liu, Alessandra Breschi, Liangliang Zhang, Pouya Kheradpour, Sylvia Li, Lisa Soleymani Lehmann, Alessandro Julianelli, Matt Edwards, Yugang Jia, David Nola, Raghav Mani, Pankaj Vats, Jesse Tetreault, T. J. Chen, and Cory Y. McLean. Integrating Genomics into Multimodal EHR Foundation Models, October 2025. arXiv:2510.23639 [cs] version: 1.

Bert Arnrich, Edward Choi, Jason A. Fries, Matthew B. A. McDermott, Jungwoo Oh, Tom J. Pollard, Nigam Shah, Ethan Steinberg, Michael Wornow, and Robin van de Water. Medical Event Data Standard (MEDS): Facilitating Machine Learning for Health. In *ICLR 2024 Workshop on Learning from Time Series for Health*, March 2024. URL <https://openreview.net/forum?id=IsHy2ebjIG>.

Søren Asmussen and Peter W. Glynn. *Stochastic Simulation: Algorithms and Analysis*, volume 57 of *Stochastic Modelling and Applied Probability*. Springer, New York, NY, 2007. ISBN 978-0-387-30679-7. doi: 10.1007/978-0-387-69033-9. URL <http://link.springer.com/10.1007/978-0-387-69033-9>.

Suhana Bedi, Jason Alan Fries, and Nigam H. Shah. How to interpret 'zero-shot' results from generative EHR models. *Nature Medicine*, January 2026. ISSN 1546-170X. doi: 10.1038/s41591-025-04094-8. URL <https://www.nature.com/articles/s41591-025-04094-8>.

Michael C. Burkhart, Bashar Ramadan, Zewei Liao, Kaveri Chhikara, Juan C. Rojas, William F. Parker, and Brett K. Beaulieu-Jones. Foundation models for electronic health records: representation dynamics and transferability. arXiv:2504.10422, 2025.

Michael C. Burkhart, Bashar Ramadan, Luke Solo, William F. Parker, and Brett K. Beaulieu-Jones. Quantifying surprise in clinical care: Detecting highly informative events in electronic health records with foundation models. In *Pacific Symposium on Biocomputing*, volume 31, pages 173–188, 2026.

Corinna Cortes, L. D. Jackel, Sara Solla, Vladimir Vapnik, and John Denker. Learning curves: Asymptotic values and rate of convergence. In J. Cowan, G. Tesauro, and J. Alspector, editors, *Advances in Neural Information Processing Systems*, volume 6. Morgan-Kaufmann, 1993. URL https://proceedings.neurips.cc/paper_files/paper/1993/file/1aa48fc4880bb0c9b8a3bf979d3b917e-Paper.pdf.

Rosa L Figueroa, Qing Zeng-Treitler, Sasikiran Kandula, and Long H Ngo. Predicting sample size required for classification performance. *BMC Medical Informatics and Decision Making*, 12(1):8, 2012. doi: 10.1186/1472-6947-12-8.

Yarin Gal and Zoubin Ghahramani. Dropout as a bayesian approximation: Representing model uncertainty in deep learning. In Maria Florina Balcan and Kilian Q. Weinberger, editors, *Proceedings of The 33rd International Conference on Machine Learning*, volume 48 of *Proceedings of Machine Learning Research*, pages 1050–1059, New York, New York, USA, 20–22 Jun 2016. PMLR. URL <https://proceedings.mlr.press/v48/gal16.html>.

Martha Gulati, Phillip D. Levy, Debabrata Mukherjee, Ezra Amsterdam, Deepak L. Bhatt, Kim K. Birtcher, Ron Blankstein, Jack Boyd, Renee P. Bullock-Palmer, Theresa Conejo, Deborah B. Diercks, Federico Gentile, John P. Greenwood, Erik P. Hess, Steven M. Hollenberg, Wael A. Jaber, Hani Jneid, José A. Joglar, David A. Morrow, Robert E. O'Connor, Michael A. Ross, and Leslee J. Shaw. 2021 AHA/ACC/AE/CHEST/SAEM/SCCT/SCMR Guideline for the Evaluation and Diagnosis of Chest Pain: Executive Summary: A Report of the American College of Cardiology/American Heart Association Joint Committee on Clinical Practice Guidelines. *Journal of the American College of Cardiology*, 78(22):2218–2261, 2021. ISSN 0735-1097. doi: <https://doi.org/10.1016/j.jacc.2021.07.052>. URL <https://www.sciencedirect.com/science/article/pii/S0735109721057946>.

Lin Lawrence Guo, Jason Fries, Ethan Steinberg, Scott Lanyon Fleming, Keith Morse, Catherine Afandilian, Jose Posada, Nigam Shah, and Lillian Sung. A multi-center study on the adaptability of a shared foundation model for electronic health records. *npj Digit. Med.*, 7, 2024.

Joel Hestness, Sharan Narang, Newsha Ardalani, Gregory Diamos, Heewoo Jun, Hassan Kianinejad, Md. Mostofa Ali Patwary, Yang Yang, and Yanqi Zhou. Deep learning scaling is predictable, empirically. *arXiv preprint arXiv:1712.00409*, 2017.

Renee Y. Hsia, Zachariah Hale, and Jeffrey A. Tabas. A National Study of the Prevalence of Life-Threatening Diagnoses in Patients With Chest Pain. *JAMA Internal Medicine*, 176(7): 1029–1032, July 2016. ISSN 2168-6106. doi: 10.1001/jamainternmed.2016.2498. URL <https://doi.org/10.1001/jamainternmed.2016.2498>.

Alistair E. W. Johnson, Tom J. Pollard, and Roger G. Mark. MIMIC-III clinical database (version 1.4), 2016.

Alistair E. W. Johnson, Lucas Bulgarelli, Lu Shen, Alvin Gayles, Ayad Shammout, Steven Horng, Tom J. Pollard, Sicheng Hao, Benjamin Moody, Brian Gow, Li-Wei H. Lehman, Leo A. Celi, and Roger G. Mark. MIMIC-IV, a freely accessible electronic health record dataset. *Scientific Data*, 10(1):1, January 2023. ISSN 2052-4463. doi: 10.1038/s41597-022-01899-x.

Zeljko Kraljevic, Dan Bean, Anthony Shek, Rebecca Bendayan, Harry Hemingway, Joshua Au Yeung, Alexander Deng, Alfred Baston, Jack Ross, Esther Idowu, James T Teo, and Richard J B Dobson. Foresight-a generative pretrained transformer for modelling of patient timelines using electronic health records: a retrospective modelling study. *Lancet Digit. Health*, 6(4), 2024.

Yikuan Li, Shishir Rao, José Roberto Ayala Solares, Abdelaali Hassaine, Rema Ramakrishnan, Dexter Canoy, Yajie Zhu, Kazem Rahimi, and Gholamreza Salimi-Khorshidi. BEHRT: Transformer for electronic health records. *Sci. Rep.*, 10, 2020.

Zhen Lin, Shubhendu Trivedi, and Jimeng Sun. Generating with confidence: Uncertainty quantification for black-box large language models, 2024. ISSN 2835-8856. URL <https://openreview.net/forum?id=DWkJCSxKU5>.

L. Julián Lechuga López, Shaza Elsharief, Dhiyaa Al Jorf, Firas Darwish, Congbo Ma, and Farah E. Shamout. Uncertainty Quantification for Machine Learning in Healthcare: A Survey, May 2025. URL <http://arxiv.org/abs/2505.02874>. arXiv:2505.02874 [cs] version: 1.

Matthew McDermott, Bret Nestor, Peniel Argaw, and Isaac S Kohane. Event stream GPT: A data pre-processing and modeling library for generative, pre-trained transformers over continuous-time sequences of complex events. In *Adv. Neural Inf. Process. Syst.*, volume 36, pages 24322–24334, 2023.

Matthew McDermott, Paweł Renc, Nassim Oufattole, Robin van de Water, Patrick Rockenschaub, Ryan King, Simon Lee, and Chao Pang. MEDS-Transforms, December 2025a. URL https://github.com/mmcdermott/MEDS_transforms. original-date: 2024-05-17T15:19:57Z.

Matthew B. A. McDermott, Haoran Zhang, Lasse Hyldig Hansen, Giovanni Angelotti, and Jack Gallifant. A closer look at auroc and auprc under class imbalance, 2025b. URL <https://arxiv.org/abs/2401.06091>.

Chao Pang, Xinzhuo Jiang, Krishna S. Kalluri, Matthew Spotnitz, RuiJun Chen, Adler Perotte, and Karthik Natarajan. CEHR-BERT: Incorporating temporal information from structured EHR data to improve prediction tasks. In *Proceedings of Machine Learning for Health*, volume PMLR 158, pages 239–260, 2021.

Laila Rasmy, Yang Xiang, Ziqian Xie, Cui Tao, and Degui Zhi. Med-BERT: pretrained contextualized embeddings on large-scale structured electronic health records for disease prediction. *npj Digit. Med.*, 4(1):86, 2021.

Paweł Renc, Yugang Jia, Anthony E. Samir, Jarosław Was, Quanzheng Li, David W. Bates, and Arkadiusz Sitek. Zero shot health trajectory prediction using transformer. *npj Digital Medicine*, 7(1):256, September 2024. ISSN 2398-6352. doi: 10.1038/s41746-024-01235-0. URL <https://www.nature.com/articles/s41746-024-01235-0>. Publisher: Nature Publishing Group.

Paweł Renc, Michał K Grzeszczyk, Nassim Oufattole, Deirdre Goode, Yugang Jia, Szymon Bieganski, Matthew B A McDermott, Jarosław Was, Anthony E Samir, Jonathan W Cunningham, David W Bates, and Arkadiusz Sitek. Foundation model of electronic medical records for adaptive risk estimation. *GigaScience*, 14:giaf107, 09 2025. ISSN 2047-217X. doi: 10.1093/gigascience/giaf107. URL <https://doi.org/10.1093/gigascience/giaf107>.

Ethan Steinberg, Ken Jung, Jason A. Fries, Conor K. Corbin, Stephen R. Pfahl, and Nigam H. Shah. Language models are an effective representation learning technique for electronic health record data. *J. Biomed. Inf.*, 113, 2021.

Ethan Steinberg, Jason Alan Fries, Yizhe Xu, and Nigam Shah. MOTOR: A time-to-event foundation model for structured medical records. In *The Twelfth International Conference on Learning Representations (ICLR)*, 2024. URL <https://openreview.net/forum?id=RDFkGZ9Dkh>. Spotlight paper.

Kiana Vu, İsmet Selçuk Özer, Phung Lai, Zheng Wu, Thilanka Munasinghe, and Jennifer Wei. From Black Box to Insight: Explainable AI for Extreme Event Preparedness, November 2025. URL <http://arxiv.org/abs/2511.13712>. arXiv:2511.13712 [cs].

Shane Waxler, Paul Blazek, Davis White, Daniel Sneider, Kevin Chung, Mani Nagarathnam, Patrick Williams, Hank Voeller, Karen Wong, Matthew Swanhorst, Sheng Zhang, Naoto Usuyama, Cliff Wong, Tristan Naumann, Hoifung Poon, Andrew Loza, Daniella Meeker, Seth Hain, and Rahul Shah. Generative medical event models improve with scale, 2025. URL <https://arxiv.org/abs/2508.12104>.

Michael Wornow, Rahul Thapa, Ethan Steinberg, Jason Alan Fries, and Nigam Shah. EHRSHOT: An EHR benchmark for few-shot evaluation of foundation models. In *Neurips Datasets and Benchmarks Track*, volume 36, pages 67125–67137, 2023a.

Michael Wornow, Yizhe Xu, Rahul Thapa, Birju Patel, Ethan Steinberg, Scott Fleming, Michael A. Pfeffer, Jason Fries, and Nigam H. Shah. The shaky foundations of large language models and foundation models for electronic health records. *NPJ digital medicine*, 6(1):135, July 2023b. ISSN 2398-6352. doi: 10.1038/s41746-023-00879-8.

Michael Wornow, Suhana Bedi, Miguel Angel Fuentes Hernandez, E Steinberg, J Fries, Christopher Ré, Oluwasanmi Koyejo, and Nigam H Shah. Context clues: Evaluating long context models for clinical prediction tasks on EHRs. In *ICLR*, 2025.

Oussama Zekri, Ambroise Odonnat, Abdelhakim Benechehab, Linus Bleistein, Nicolas Boulle, and Ievgen Redko. Large language models as markov chains, 2025. URL <https://openreview.net/forum?id=RDFkGZ9Dkh>.

Appendix A. Nomenclature

M_0 Equation shorthand for the Monte Carlo estimator.

\mathcal{S} Equation shorthand for the SCOPE estimator.

\mathcal{R} Equation shorthand for the REACH estimator.

T_O The random variable equal to the index of the first outcome of interest token.

T_E The random variable equal to the index of the terminating token of a sequence or the token coming after the first outcome of interest token.

A The event describing the subset of timelines in the first probability space that contain the outcome of interest token.

B The event describing the subset of timelines that have a successful Bernoulli trial under the second probability space.

V The vocabulary of tokens.

O The outcome of interest token, an element of V .

$X_{1:n}$ A tokenized timeline of length n .

$\hat{X}_{1:n}$ A tokenized timeline of length n that excludes O from the set of possible next tokens.

Ω_{M_τ} The probability space of timelines sampled under some model M and time limit τ .

Ω_\emptyset The probability space of outcome-free timelines and Bernoulli trials at each token.

$\mathbf{c}_{1:n}$ The result of n Bernoulli trials for some outcome-free tokenized timeline of length n .

Appendix B. Proof of Equal Probabilities

Consider a sequence generation model M that generates a probability distribution for the next token from some vocabulary V , which contains our outcome of interest token O . Let $Y_{1:n}$ denote the sequence of tokens that the model has processed before generating any new tokens. Note that each token that is associated with an increasing time stamp \mathcal{T}_i . Let $P_M(Y_0 = t_j)$ denote the probability that the next token generated by the model is t_j . Likewise, if the model has already generated $Y_{1:i}$, $P_M(Y_{i+1} = t_j|Y_{1:i})$ denotes the probability that the next token generated will be t_j .

Before introducing our improved sampling method, we will introduce the standard Monte Carlo method. Define probability space Ω_{M_τ} :

$$\Omega_{M_\tau} := \{X_{1:n} \mid \forall i \in [n], X_i \in V, \mathcal{T}_i < \tau\} \quad (5)$$

$$P_{\Omega_{M_\tau}}(X_{1:n}) = P_M(Y_0 = X_0) \prod_{i=1}^n P_M(Y_i = X_i | Y_{1:i-1} = X_{1:i-1}) \quad (6)$$

Intuitively, the samples in this probability space correspond to the sequences of tokens generated by sampling the tokens directly at the rate dictated by the model. Within this distribution, define the event A :

$$A := \{X_{1:n} \in \Omega_{M_\tau} \mid \exists i \in [n] \text{ s.t. } X_i = O\} \quad (7)$$

Next, consider a second probability space Ω_ϕ :

$$\Omega_\phi := \{(X_{1:n}, \mathbf{c}_{1:n}) \mid \forall i \in [n], X_i \in V \setminus O, \mathcal{T}_i < \tau, \mathbf{c}_i \in \{0, 1\}\} \quad (8)$$

$$P_{\Omega_\phi}(X_{1:n}) = \left(\frac{P_M(Y_0 = X_0)}{P_M(Y_0 \neq O)} \prod_{i=1}^n \frac{P_M(Y_i = X_i | Y_{1:i-1} = X_{1:i-1})}{P_M(Y_i \neq O | Y_{1:i-1} = X_{1:i-1})} \right) \quad (9)$$

Intuitively, this can be understood as the probability of generating a given sequence $X_{1:n}$ by sampling next tokens at the rates suggested by the model but this time **excluding** the outcome token.

Define $h_i(X_{1:n}) = P_M(Y_i = O | X_{1:i-1})$

(Note that in order to keep notation simple $X_{1:n}$ may be omitted)

$$P_{\Omega_\phi}(X_{1:n}, \mathbf{c}_{1:n}) = P_{\Omega_\phi}(X_{1:n}) \prod_{i=1}^n \left((1 - \mathbf{c}_i)(1 - h_i) + \mathbf{c}_i h_i \right) \quad (10)$$

Each \mathbf{c}_i can be understood as an independent Bernoulli trial with probability h_i . The purpose of these variables is to simulate the tokens in the timeline being randomly “flipped” to the outcome token.

Now define the event corresponding to all outcomes where at least one token in the timeline is randomly flipped to the outcome of interest as B .

Consider the complements of our two events described above: A^C , which corresponds to all sampled timelines that **do not** contain the outcome of interest token, and B^C , which corresponds to all sampled timelines where **none** of the Bernoulli trials succeed and flip a token to the outcome of interest.

Since the elements of both probability spaces are determined by the same next token distribution model, note that there exists a natural bijection $\phi: A^C \rightarrow B^C$:

$$\phi(X_{1:n}) := (X_{1:n}, (0, \dots, 0)) \quad (11)$$

Furthermore, from our definition of our probability spaces:

$$P_{\Omega_\phi}(\phi(X_{1:n})) = P_{\Omega_\phi}((X_{1:n}, (0, \dots, 0))) \quad (12)$$

Looking at the definitions once more, it is clear that the Bernoulli trial product terms from (10) cancel with the denominator of (9) to yield exactly (6). Therefore:

$$P_{\Omega_\varnothing}(\phi(X_{1:n})) = P_{\Omega_{M_\tau}}(X_{1:n}) \quad (13)$$

By the definition of the probability of an event, this allows for the substitution:

$$P_{\Omega_\varnothing}(B^C) = \sum_{(X_{1:n}, (0, \dots, 0)) \in B^C} P_{\Omega_\varnothing}((X_{1:n}, (0, \dots, 0))) \quad (14)$$

$$= \sum_{X_{1:n} \in A^C} P_{\Omega_\varnothing}(\phi(X_{1:n})) = \sum_{X_{1:n} \in A^C} P_{\Omega_{M_\tau}}(X_{1:n}) = P_{\Omega_{M_\tau}}(A^C) \quad (15)$$

So, by the law of total probability, we have shown that $P(A) = P(B)$.

Appendix C. Proof of $\text{Var}(\mathcal{R}) \leq \text{Var}(\mathcal{S})$

From the body of the paper, recall that we can define our SCOPE estimator as

$$\mathcal{S} = \frac{1}{n} \sum_{i=1}^n \left[\sum_{t=1}^{\min\{T_E(X^{(i)}), T_O(X^{(i)})\}} P(X_t = O | X_{1:t-1}^{(i)}) \right] \quad (16)$$

If we then define

$$f_t(x) = P(X_T = O | X_{1:t-1} = x_{1:t-1}) \mathbb{1}_{\{T_O(x_{1:t-1}), T_E(x) > t-1\}} \quad (17)$$

We can instead express \mathcal{S} as:

$$\mathcal{S} = \frac{1}{n} \sum_{i=1}^n \sum_{t \geq 1} f_t(X^{(i)}) \quad (18)$$

As an alternative to our previous derivation of the REACH estimator, let \hat{P} denote the restriction of P to $V \setminus \{O\}$ and apply importance sampling to (16) to obtain:

$$\mathcal{R} = \frac{1}{n} \sum_{i=1}^n \left[\sum_{t=1}^{T_E(\hat{X}^{(i)})} P(X_t = O | \hat{X}_{1:t-1}^{(i)}) \frac{P(\hat{X}^{(i)}_{1:t-1})}{\hat{P}(\hat{X}^{(i)}_{1:t-1})} \right] \quad (19)$$

where $\forall i \in [n]$, $X^{(i)} \sim^{\text{i.i.d.}} \hat{P}$. For any sequence x in the vocabulary $V \setminus \{O\}$, we have

$$\begin{aligned} \hat{P}(X_{1:t-1} = x_{1:t-1}) &= \prod_{j=1}^{t-1} \hat{P}(X_j = x_j | X_{1:j-1} = x_{1:j-1}) \\ &= \prod_{j=1}^{t-1} \frac{P(X_j = x_j | X_{1:j-1} = x_{1:j-1})}{1 - P(X_j = O | X_{1:j-1} = x_{1:j-1})} \end{aligned}$$

so that

$$\frac{P(\hat{X}_{1:t-1}^{(i)})}{\hat{P}(\hat{X}_{1:t-1}^{(i)})} = \prod_{j=1}^{t-1} (1 - P(X_j = O | X_{1:j-1} = x_{1:j-1})) \quad (20)$$

which, when substituted into (19), yields our original expression for \mathcal{R} provided in the body.

Define

$$h_t^0(x) = \prod_{j=1}^{t-1} (1 - P(X_j = O | X_{1:j-1} = x_{1:j-1})) \quad (21)$$

$$h_t(x) = P(X_t = O | X_{1:t-1} = x_{1:t-1}) \mathbb{1}_{\{T_E(x) > t-1\}} h_t^0(x) \quad (22)$$

Using these definitions, \mathcal{R} can be simplified as:

$$\mathcal{R} = \frac{1}{n} \sum_{i=1}^n \sum_{t \geq 1} h_t(\hat{X}^{(i)}) \quad (23)$$

Next, using our result from (20):

$$\mathbb{E}[h_t(\hat{X})^2] = \int h_t(\hat{x}_{1:t}) \hat{p}(\hat{x}_{1:t}) d\hat{x}_{1:t} \quad (24)$$

$$= \int h_t(\hat{x}_{1:t}) \frac{\hat{p}(\hat{x}_{1:t})}{p(x_{1:t})} p(x_{1:t}) d\hat{x}_{1:t} \quad (25)$$

$$= \int f_t(\hat{x}_{1:t})^2 h_t^0(x_{1:t})^2 \frac{1}{h_t^0(\hat{x}_{1:t})} p(x_{1:t}) d\hat{x}_{1:t} = \mathbb{E}[f_t(X)^2 h_t^0(X)] \quad (26)$$

Since $0 \leq h_s(x) \leq 1$, we can conclude that:

$$\mathbb{E}[h_t(\hat{X})^2] \leq \mathbb{E}[f_t(X)^2] \quad (27)$$

Since \mathcal{S} and \mathcal{R} have the same expectation as unbiased estimators of the same probability, (27) demonstrates that:

$$\text{Var}(h_t(\hat{X})) \leq \text{Var}(f_t(\hat{X})) \quad (28)$$

Next, for $s < t$, we have

$$\text{Cov}(h_s(\hat{X}), h_t(\hat{X})) = \mathbb{E}[h_s(\hat{X})h_t(\hat{X})] - \mathbb{E}[h_s(\hat{X})]\mathbb{E}[h_t(\hat{X})] \quad (29)$$

By a nearly identical argument to the one presented in (24) to (26), it can be shown that

$$\begin{aligned} \mathbb{E}[h_s(\hat{X})h_t(\hat{X})] - \mathbb{E}[h_s(\hat{X})]\mathbb{E}[h_t(\hat{X})] &= \mathbb{E}[f_s(X)f_t(X)h_s^0(X)] - \mathbb{E}[f_s(X)]\mathbb{E}[f_t(X)] \\ \text{Cov}(h_s(\hat{X}), h_t(\hat{X})) &\leq \text{Cov}(f_s(X), f_t(X)) \end{aligned} \quad (30)$$

And, by (18) and (23), we reach our final conclusion that:

$$\text{Var}(\mathcal{R}) \leq \text{Var}(\mathcal{S})$$

Appendix D. Counterexample demonstrating the impossibility of a positive bound M such that if $P(A) < M$ then $\text{Var}(M_0) > \text{Var}(\mathcal{S})$ for all models and stopping conditions

In the body, it was demonstrated that $\text{Var}(\mathcal{S})$ is not necessarily less than $\text{Var}(M_0)$. Specifically, timelines for which the \mathcal{S} sub-estimator predicts an estimate for the value of the probability above 1 contribute to the inequality $\text{Var}(M_0) < \text{Var}(\mathcal{S})$. Given this fact, it seemed plausible that there could exist some positive lower bound M for the probability of the outcome of interest, $P(A)$, for which the following could hold: for any model and stopping condition, if $P(A) < M$ then $\text{Var}(\mathcal{S}) < \text{Var}(M_0)$. Such a bound would be quite useful as it would allow you determine that \mathcal{S} would be a lower variance estimator than M_0 based on the probability of the outcome alone.

However, this fact is not true and is shown to be false by the following counterexample.

Consider the following model and stopping condition. At first, the model has two possible token outputs A and B . Let it generate token A with arbitrary probability p , and B otherwise. Neither contribute toward the time limit or are the outcome of interest. The model then operates according to the following rules:

- If A was generated at the first step:
- Immediately terminate the timeline without generating any further tokens.
- If B was generated at the first step:
- Generate new tokens with equal probability of it being token H or token T . Terminate either after 3 tokens are generated or after the appearance of the first heads.

For this counterexample, we will treat H as the outcome of interest token. Naturally:

$$P(H \in X) = \frac{7}{8}(1-p) \quad (31)$$

Since \mathcal{S} and M_0 are unbiased estimators for this probability, this likewise is the expectation of both of these random variables. In order to compute the difference in variance between \mathcal{S} and M_0 , we can proceed directly from the definition of variance and the unbiasedness of our estimators:

$$\text{Var}(\mathcal{S}) - \text{Var}(M_0) = \mathbb{E}(\mathcal{S}^2) - \mathbb{E}(M_0^2) \quad (32)$$

From the table:

Outcome	Probability	M_0^2 contribution	\mathcal{S}^2 contribution
A	p	0	0
BH	$\frac{1}{2}(1-p)$	1	$\frac{1}{4}$
BTH	$\frac{1}{4}(1-p)$	1	1
BTTH	$\frac{1}{8}(1-p)$	1	$\frac{9}{4}$
BTTH	$\frac{1}{8}(1-p)$	0	$\frac{9}{4}$

$$\mathbb{E}(M_0^2) = \frac{7}{8}(1-p)$$

$$\mathbb{E}(\mathcal{S}^2) = \frac{15}{16}(1-p)$$

$$\text{Var}(\mathcal{S}) - \text{Var}(M_0) = \frac{1}{16}(1-p) \quad (33)$$

Note that if $p < 1$, (33) implies $\text{Var}(\mathcal{S}) - \text{Var}(M_0) > 0$. Further, if we allow p get arbitrarily close to 1, $P(H \in X) \rightarrow 0$, while the variance of \mathcal{S} remains strictly worse than the variance of M_0 . This shows that there cannot exist a positive value M that guarantees that if $P(H \in X) < M$ then $\text{Var}(\mathcal{S}) < \text{Var}(M_0)$.

Appendix E. Total Inference Time Reductions

In order to compute the amount of GPU time required, the total run times of our 32 data splits for the hospital mortality task using the M2 estimator were summed.

Table 1: Runtime Summary for ethos_M2_ed_4334712 (Files 0-31)

File Index	Runtime (H:MM:SS)
0	6:54:45
1	6:32:39
2	6:49:25
3	7:31:00
4	6:40:11
5	6:48:31
6	6:56:42
7	7:39:13
8	6:44:45
9	5:57:16
10	8:22:20
11	6:04:10
12	6:59:03
13	7:31:58
14	6:44:37
15	7:57:52
16	7:54:19
17	7:22:43
18	7:03:45
19	7:39:57
20	6:35:22
21	8:16:21
22	7:26:34
23	7:09:57
24	7:43:19
25	7:45:51
26	6:52:54
27	7:01:50
28	7:54:10
29	6:31:27
30	6:39:40
31	6:54:19
Total	164:33:28

Next, in order to estimate the time required by the standard ETHOS-ARES library, the inference code was left to run with 8xA100 GPUS for 1 hour. This generated 22395 samples out of the required 4304700. This implies a little over 192 hours will be required to complete inference using this setup. Multiplying by 8 to determine the GPU hours required, we get over 1537 GPU hours. This yields a total speedup factor:

$$\frac{1537.74}{164.55} = \boxed{9.35}$$

Note that this does not include any speedups from the reductions in the number of samples required for equivalent performance between methods. For the sake of transparency, the log files that contain these measurements are made available in the codebase.

Appendix F. Hospital Mortality: Performance vs Sample Count Plots and P-Values

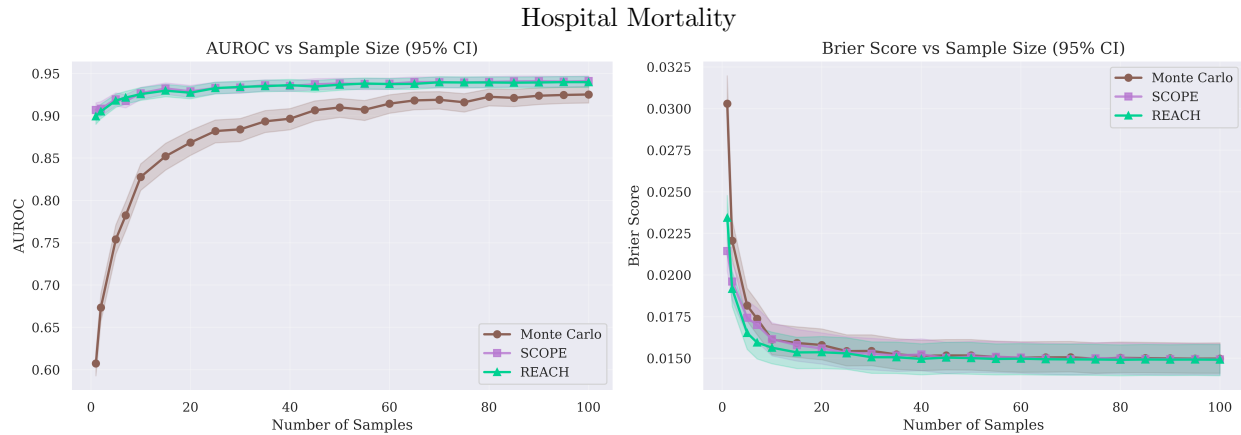


Table 2: Hospital Mortality prediction performance comparison

Method	Number of Samples	ROC-AUC	Brier Score
Monte Carlo	100	0.925 [0.915, 0.935]	0.015 [0.014, 0.016]
SCOPE	11	0.926 [0.919, 0.934]	0.016 [0.015, 0.017]
REACH	10	0.925 [0.917, 0.932]	0.016 [0.015, 0.017]
<i>One-sided permutation test p-values</i>			
MC vs SCOPE	-	0.550	0.030
MC vs REACH	-	0.477	0.135

Appendix G. ICU Admission: Performance vs Sample Count Plots and P-Values

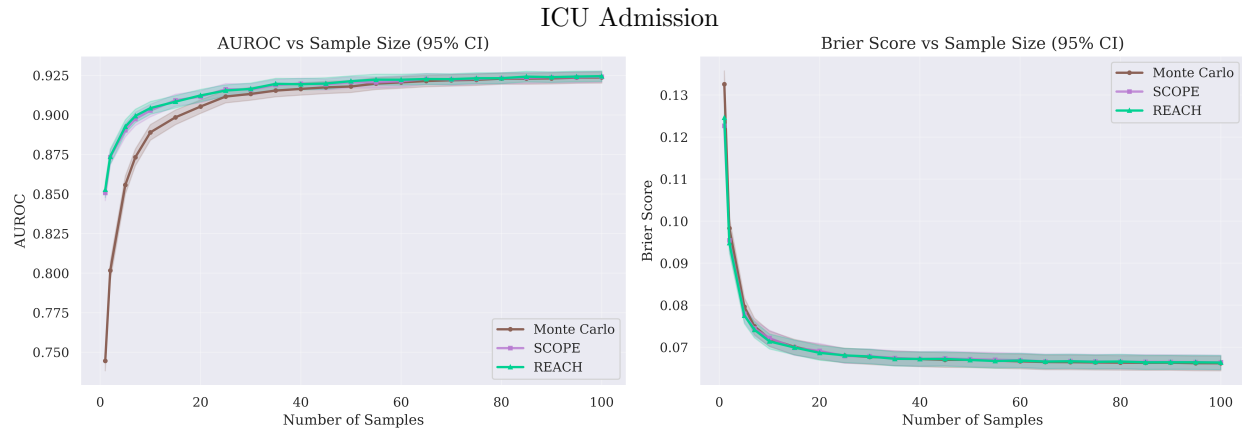


Table 3: ICU Admission prediction performance comparison

Method	Number of Samples	ROC-AUC	Brier Score
Monte Carlo	100	0.924 [0.920, 0.927]	0.066 [0.065, 0.068]
SCOPE	89	0.923 [0.920, 0.927]	0.066 [0.065, 0.068]
REACH	82	0.923 [0.920, 0.927]	0.067 [0.065, 0.068]
<i>One-sided permutation test p-values</i>			
MC vs SCOPE	-	0.453	0.411
MC vs REACH	-	0.407	0.404

Appendix H. Dispersion of Estimates Computation

Consider some outcome with general prevalence of $1/10000$. Next, we want to consider the probability that a patient with $10\times$ the general population risk is assigned a risk score by the Monte Carlo estimator that exceeds the risk score of a patient with risk equal to the prevalence.

The PMF for the Binomial distribution is

$$f(k; n, p) = \binom{n}{k} p^k (1-p)^{n-k}.$$

In order to compute the probability that the higher risk patient is ranked higher, we sum over all possible outcomes for the average risk patient and multiply each by the probability that the higher risk patient generates more samples that indicate the outcome of interest:

$$\sum_{k=0}^{100} f(k; 100, \frac{1}{10000}) \cdot \sum_{j=k+1}^{100} f(j; 100, \frac{1}{1000}) = 0.0943.$$

Thus there is only a 9.43% chance that a patient with risk $10\times$ baseline is given a higher risk score than a patient with average risk.